Acta of Bioengineering and Biomechanics
Vol. 19, No. 4, 2017

Original paper
DOI: 10.5277/ABB-00949-2017-02

Elastic constants influence on the L4-L5-S1 annuli fibrosus behavior, a probabilistic finite element analysis

HECTOR E. JARAMILLO[1,*], JOSE J. GARCIA[2]

[1] Universidad Autonoma De Occidente, Colombia.
[2] Universidad del Valle, Colombia.

Purpose: A probabilistic finite element (FE) analysis of the L4-L5 and L5-S1 human annulus fibrosus (AF) was conducted to obtain a better understanding of the biomechanics of the AF and to quantify its influence on the range of motion (ROM) of the L4-L5 and L5-S1 segments. *Methods:* The FE models were composed of the AF and the upper and lower endplates. The AF was represented as a continuous material composed of a hyperelastic isotropic Yeoh matrix reinforced with two families of fibers described with an exponential energy function. The caudal endplate was fully restricted and 8 Nm pure moment was applied to the cranial endplate in flexion, extension, lateral flexion and axial rotation. The mechanical constants were determined randomly based on a normal distribution and average values reported. *Results:* Results of the 576 models show that the ROM was more sensitive to the initial stiffness of the fibers rather than to the stiffening coefficient represented in the exponential function. The ROM was more sensitive to the input variables in extension, flexion, axial rotation and lateral bending. The analysis showed an increased probability for the L5-S1 ROM to be higher in flexion, extension and axial rotation, and smaller in lateral flexion, with respect to the L4-L5 ROM. *Conclusions:* An equation was proposed to obtain the ROM as a function of the elastic constants of the fibers and it may be used to facilitate the calibration process of the human spine segments and to understand the influence of each elastic constant on the ROM.

Key words: *finite element analysis, hyperelastic, range of motion, intervertebral discs, probabilistic analysis, sensitivity factor*

1. Introduction

The uncertainty in loads, geometry and material properties is present in the theoretical research of the spine. However, a few studies [7], [16], [18], [21], [22], [25]–[28] have accomplished probabilistic analysis in order to estimate the influence of these variations [15] on the mechanical response of the spine [14].

In one of the studies Spilker et al. [25]–[27] used a model of the spine under axial compressive load to find that increases in the disc height and the ratio of the nucleus area to disc area cause a reduction of the intradiscal pressure (IDP), the bulge, and the vertical displacement of the disc. Rao et al. [21] used a disc model of the L5-S1 segment to determine that the Young's modulus and Poisson's ratio of the ground matrix play an important role in the biomechanics of the segment, while the changes in the mechanical properties of the cortical bone, the cancellous bone, the endplates, and the nucleus pulposus have marginal effects. Fagan et al. [7] found that the properties of the fibers of the annulus fibrosus have no significant effect on the disc stiffness under compression, but it affects the flexural and torsional properties.

Malandrino et al. [16] considered the pore-elastic effect between the annulus, nucleus pulposus, articular cartilage, and trabecular bone to conclude that the permeability is an important factor that has an influence on the vertical displacements during compression, the IDP in compression and torsion, the pore

* Corresponding author: Hector Enrique Jaramillo, Universidad Autonoma De Occidente, Calle 15A # 67-35 Apto 403A, 760033 Cali (Valle), Colombia. Tel. 573006092053, e-mail: hjsuarez@uao.edu.co

Received: July 7th, 2017
Accepted for publication: September 1st, 2017

pressure in torsion and the speed of fluid leaving through the vertebral bodies.

Rohlmann et al. [22] used a L3-L5 lumbar segment to analyze the effect of the position and radius of a ball implant, the presence of injured tissue, and the space between the facets capsules in the ROM, the IDP and the contact forces between the facet capsules. They found that the ROM presents a strong variations for different combinations of input parameters. Niemeyer et al. [18] used a simplified model of the L3-L4 segment to determine that the disc height, width, thickness and position of the facet joints have a great impact over intradiscal pressure, range of motion and facet joint contact forces. Finally, Thacker et al. [28] used a model of the C4-C6 segment to conclude that the most important variables in the probabilistic response are the modulus of elasticity of the annulus fibrosus and the force-displacement curves of the flavum ligament, interspinous ligament and the capsular ligaments.

None of the aforementioned studies have addressed the influence of the elastic constants of the annulus in the segment response. To obtain a better understanding of the biomechanics of the annulus, this paper presents a probabilistic analysis of L4-L5 and L5-S1 annuli fibrosus. Particularly, the influence of the elastic constants of the annulus fibrosus on the ROM in flexion, extension, lateral bending and axial rotation was assessed.

2. Materials and methods

2.1. Geometry

The annulus fibrosus and the upper and lower endplates (Figs. 1–2) of a finite element model of the L4-L5 and L5-S1 segments reported by Jaramillo et al. [12] were used in the analysis.

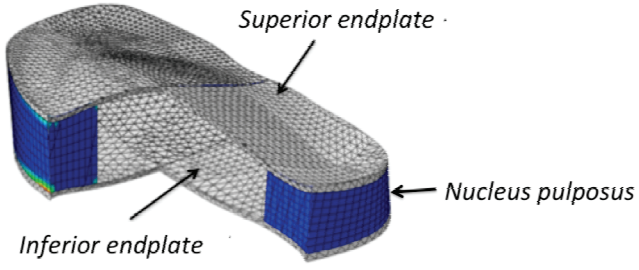

Fig. 1. Sectional view of the model of the annulus fibrosus and endplates

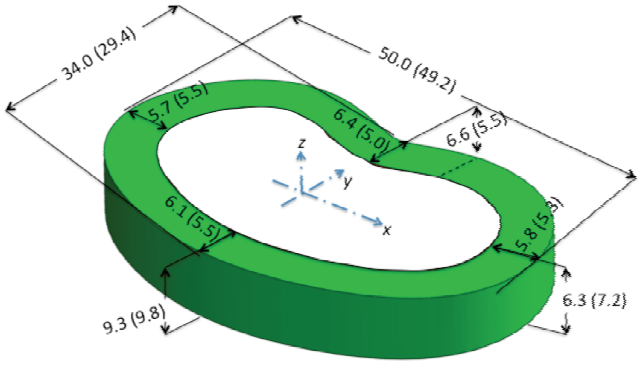

Fig. 2. Dimensions in mm of the L4-L5 (outside the parenthesis) and L5-S1 (inside the parenthesis) intervertebral discs

2.2. Mechanical properties and constitutive equations

The vertebrae and the endplates were assumed to be rigid. This simplification is supported by previous studies [5], [17] which showed that a model with rigid vertebrae predicts maximum stress values in the disc that are only 2% different from those obtained with a model including the flexibility of the bone. This simplification enabled to apply the pure moments on the endplates and represented a significant reduction of computational time [5], [17]. According to other studies [1], [19], the annulus was represented as a matrix reinforced with two families of fibers, where the following hyperelastic Yeoh function was used for the matrix,

$$W_m = c_1(I_1 - 3) + c_2(I_1 - 3)^2 + c_3(I_1 - 3)^3, \qquad (1)$$

where c_1, c_2, c_3, are material constants and I_1 is the first deviatoric invariant of the Green deformation tensor.

For the fibers, the following exponential function was included, which was consistent with previous studies [1], [12],

$$W_f = \frac{a_1}{a_2}[e^{a_2(I_4-1)^2} + e^{a_2(I_6-1)^2} - 2], \qquad (2)$$

where a_1, a_2 are material constants and I_4 and I_6 are the deviatoric invariants associated with the two families of fibers, which are defined as:

$$I_4 = N^{(1)} C N^{(1)} \qquad (3)$$

$$I_6 = N^{(2)} C N^{(2)} \qquad (4)$$

where $N^{(1)}$ and $N^{(2)}$ are the unit vectors along the two fiber directions in the non-deformed configuration,

Table 1. Constants a_1 and a_2 randomly obtained

	Mean	DS	Random values (Normal distribution)									
a_1 [MPa]	0.23	0.15	0.185	0.038	0.267	0.421	0.410	0.490	–0.09	0.195	0.394	0.067
a_2	7.44	7.5	12.064	–3.90	13.177	13.657	15.889	20.929	–0.99	9.549	12.734	6.579

and C is the deviatoric right Green deformation tensor. Note that the constant a_1 is proportional to the initial stiffness of the fibers, while the constant a_2 represents the degree of stiffening with strain. The reinforcing fibers were assumed to be stressed only under a positive strain. A subroutine Uanisohyper of the program ABAQUS was developed to implement the aforementioned energy functions.

A constant fiber orientation of 30° [6], [24], [30] with respect to the transverse plane was assumed. The mechanical constants of the matrix (c_1 = 0.035 MPa, c_2 = 0.00065 MPa and c_3 = 0.00045 MPa) from a calibrated model of the L4-L5-S1 segment reported by Jaramillo et al. [12] were assumed in calculations. For the probabilistic analysis, the elastic constants a_1 and a_2 of the annulus were determined randomly using Excel "Data\Data Analysis\Random number generation" (www.microsoft.com/, USA) according to a normal distribution based on data reported by Cortes et al. [4] (Table 1). The constants a_1 and a_2 were combined to obtain a set of 100 data.

2.3. Boundary conditions and loads

The caudal endplate was fully restricted and a ramped pure moment was applied to the cranial endplate from 0 to 8 Nm for each kind of movement (flexion, extension, lateral bending and axial rotation). The combination of the 100 elastic constants, the four movements and two discs (segments L4-L5 and L5-S1) yielded a total of 800 models, out of which 224 were excluded due to negative values of a_1 and a_2.

The software Abaqus 6.14.2 (Dassault Systemes SA, Waltham, Massachusetts, USA, http://www.3ds.com/products-services/simulia/) was used in the analyses. Tridimensional hybrid hexahedral elements with eight nodes (C3D8H) and tetrahedral (C3D10) were used to represent the annulus fibrosus and the endplates, respectively. Since the annulus was assumed to be incompressible, it was necessary to use hybrid elements (C3D8H), as required by the UANISOHYPER routine. Since different type of elements represented the annulus fibrosus and the endplates, the Tie option was used to connect the parts.

2.4. Convergence analysis

The L4-L5 segment annulus fibrosus disc was selected for convergence analysis. The experimental properties reported by Cortes et al. [4] and five meshes (M1, M2, M3, M4 and M5) were used in the convergence analysis (Table 2). The boundary conditions and loads were equal to those explained in 2.3.

Table 2. Different mesh size used in the convergence analysis, all models used 8-node hexahedral elements (C3D8H)

Model	Elements number	Total nodes	Degree of Freedom (DOF)
M1	522	30978	91896
M2	1580	33478	97280
M3	5250	41778	114840
M4	9472	50988	134026
M5	11304	54962	142284

The percentage difference for the *ROM* decreased along with an increasing number of elements (Fig. 3). The ROM stabilized from the M4 mesh, where the ROM differences with respect to the M5 mesh were 0.5% in flexion, 0.8% in extension, 0.4% in lateral bending, and 0.5% in axial rotation. Hence, the M4 mesh consisting of 9472 elements was selected for the analysis. Each model was analyzed in a relatively reduced time (1781–2727 s) in a workstation DELL X5690.

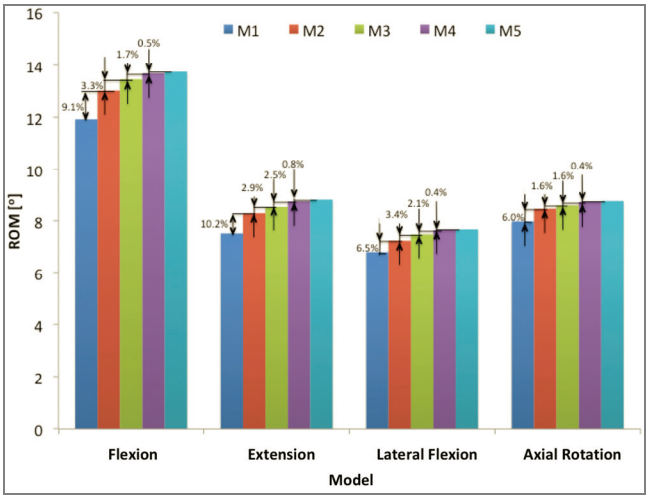

Fig. 3. Convergence analysis based on the *ROM*

The final mesh of the disc had eight divisions along its axial and radial directions.

2.5. Procedure to analyze the results

First, the ROM was compared with experimental data reported in a previous work, and obtained in the last stage of the stepwise reduction method [13]. Next, the surface response of ROM versus a_1 and a_2 was plotted and several equations were considered as candidates to fit this response. The fit was evaluated using a nonlinear least squares regression. The cumulative probability and probability density function were obtained using Origin 8.5 software (Northampton, UK, http://www.originlab.com).

Additionally, the ROM sensitivity to each of the input random variables (a_1, a_2) was calculated according to the equation proposed by Thacker et al. [28], [29]:

$$\alpha_i = \frac{\partial \beta}{\partial u_i}, \tag{3}$$

where α_i is the sensitivity, β is the output variable (*ROM*) and u_i is the input variable (a_1, a_2).

Finally, the coefficient of variation (*CV*) for the *ROM* was calculated as a measure of the results dispersion.

3. Results

The ROM versus moment behavior was obtained and compared with the experimental *ROM* [13], for the L4-L5 segment in flexion (Fig. 4a), in extension (Fig. 4b), in lateral flexion (Fig. 4c) and in axial rotation (Fig. 4d), and for the L5-S1 segment in flexion (Fig. 5a), in extension (Fig. 5b), in lateral flexion (Fig. 5c) and in axial rotation (Fig. 5d). The ROM dispersion (Fig. 4) for the segment L4-L5 was greater in axial rotation (*CV* = 14.6%) and extension (*CV* = 12.6%) followed by lateral flexion (*CV* = 8.7%), and flexion (*CV* = 6.3%). For the L5-S1 segment (Fig. 5) the highest dispersion was observed in axial rotation

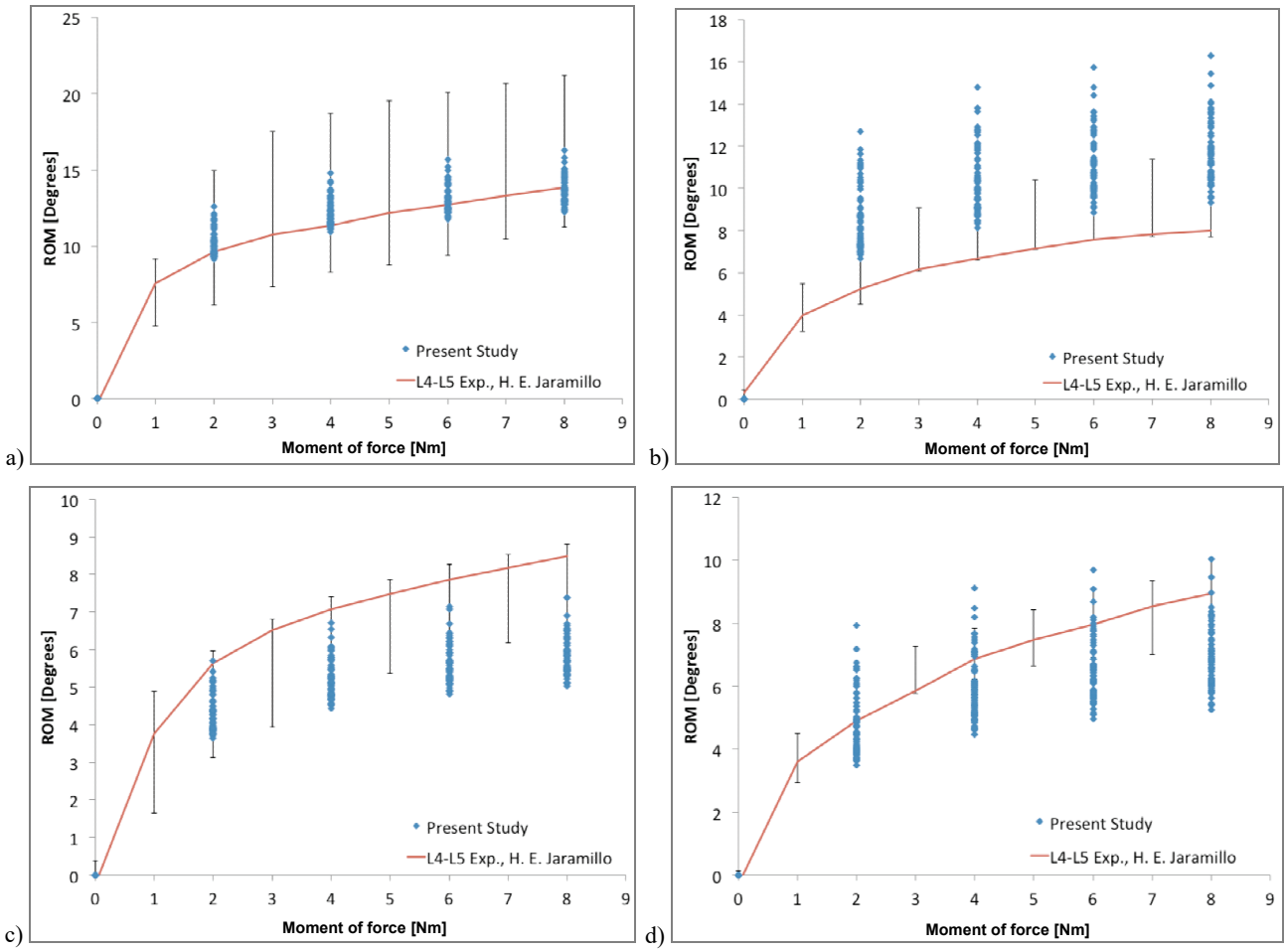

Fig. 4. Results for the L4-L5 disc compared with the experimental *ROM* [13] for:
a) flexion, b) extension, c) lateral flexion, d) axial rotation. Error bars show the experimental range

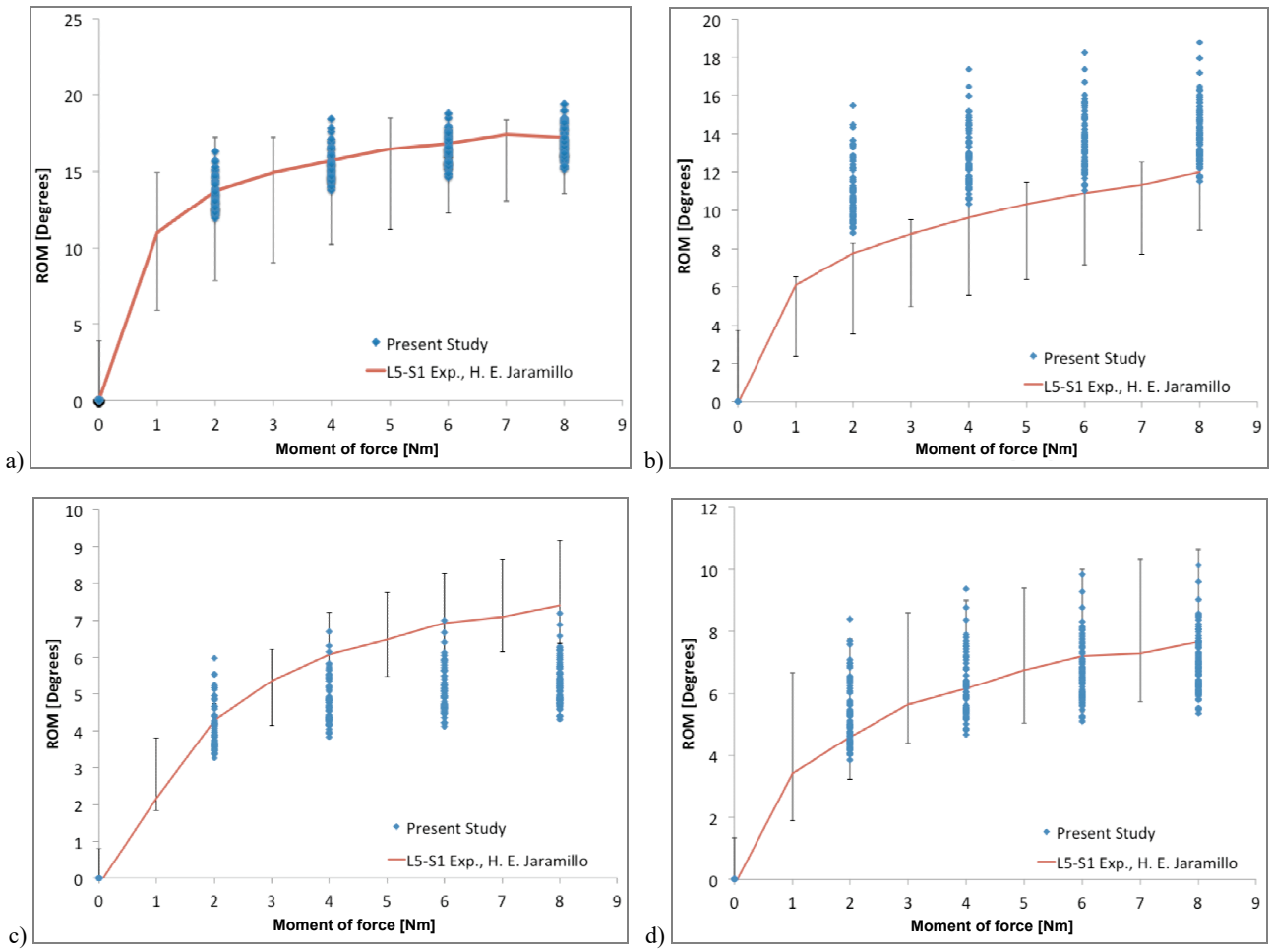

Fig. 5. Results for the L5-S1 disc compared with experimental *ROM* [13] for:
a) flexion, b) extension, c) lateral flexion, d) axial rotation. Error bars show the experimental range

(*CV* = 14.0%), followed by lateral flexion (*CV* = 11.5%), extension (*CV* = 10.6%), and flexion (*CV* = 5.6%). The *CV* for the *ROM* of both segments was lower than the *CV* of the input variable a_2 (100%) and of the same order of magnitude that the *CV* (6.5%) for the input variable a_1. The relatively low dispersion for the *ROM* under important variations of a_2 indicates a low sensitivity of *ROM* to this input variable.

With respect to the percentage of ROM results within the experimental range, it was 100% in flexion, 50% in lateral flexion, 48.3% in extension, and 25.7% in axial rotation for the L4-L5 disc. For the L5-S1 disc, these percentages were 95.9%, 94.2%, 38.0% and 15.8% for flexion, axial rotation, lateral flexion, and extension, respectively.

Several equations (Chebyshev2D, Cosine, Dose -Resp2D, Extreme2D, ExtremeCum, Fourier2D, Exponential and Gauss2D) available in the Origin software were tested to fit the ROM surface as a function of a_1 and a_2 for each movement and segment. Finally, the exponential Equation (4) yielded the best fitting with coefficients of determination (R^2) of 0.985 for the L4-L5, and 0.976 for the L5-S1 segment (Table 3).

$$ROM = Zo + Be^{\left[-\frac{a_1}{C}-\frac{a_2}{D}\right]}. \quad (4)$$

The coefficients Z_0, B and C of Eq. (4) were between 5% and 31% higher for the L5-S1 segment with respect to those for the L4-L5 segment, while D showed an opposite trend in extension, lateral flexion and axial rotation (Table 3). The response surfaces are shown in Fig. 6 for the flexion movement and different values of moment of force and are also compared with results of the parametric analysis in Fig. 7.

The *ROM* was approximately 25 times more sensitive to a_1 than to a_2 (Fig. 8). In their order, the *ROM* was more sensitive to the input variables in extension, flexion, axial rotation and lateral bending. The negative sign of the sensitivity parameter indicates that an increment in the input variables (a_1 and a_2) causes a reduction of the range of motion.

Table 3. Constants of equation (4) that fit the results of the parametric analyses

Segment	Movement	*M* [Nm]	*Zo* [Deg.]	*B* [Deg.]	*C* [MPa]	*D*	Statistical	
							Chi-Square	R^2
L4-L5	Flexion	2	8.974	5.423	0.232	24.903	0.003	0.995
		4	10.620	6.446	0.316	19.228	0.009	0.988
		6	11.251	6.952	0.386	17.757	0.013	0.982
		8	11.567	7.245	0.452	17.474	0.015	0.980
	Extension	2	6.465	9.486	0.218	23.817	0.010	0.995
		4	7.680	11.417	0.294	17.912	0.027	0.988
		6	8.135	12.192	0.365	16.569	0.037	0.983
		8	8.391	12.624	0.424	16.043	0.043	0.980
	Lateral flexion	2	3.538	3.275	0.236	24.053	0.001	0.995
		4	4.245	3.984	0.321	17.983	0.003	0.988
		6	4.536	4.285	0.389	16.330	0.004	0.983
		8	4.713	4.473	0.438	15.421	0.005	0.979
	Axial Rotation	2	3.320	7.234	0.223	20.717	0.005	0.995
		4	4.099	8.202	0.315	16.493	0.013	0.988
		6	4.411	8.619	0.390	15.512	0.017	0.983
		8	4.458	8.710	0.482	16.147	0.045	0.955
L5-S1	Flexion	2	11.681	6.980	0.267	22.579	0.008	0.992
		4	13.169	8.005	0.387	19.146	0.017	0.984
		6	13.592	8.343	0.511	19.692	0.021	0.977
		8	13.877	8.652	0.594	19.607	0.023	0.975
	Extension	2	8.421	11.134	0.276	18.982	0.020	0.991
		4	9.485	12.551	0.397	16.483	0.039	0.983
		6	9.918	13.204	0.482	15.839	0.046	0.979
		8	10.197	13.613	0.544	15.488	0.050	0.977
	Lateral flexion	2	3.104	4.389	0.263	20.817	0.006	0.984
		4	3.458	4.966	0.399	17.713	0.014	0.963
		6	3.576	5.193	0.504	17.277	0.020	0.947
		8	3.651	5.335	0.582	17.065	0.024	0.935
	Axial Rotation	2	3.620	7.728	0.263	18.005	0.008	0.993
		4	4.178	8.524	0.385	15.432	0.016	0.984
		6	4.414	8.886	0.472	14.783	0.019	0.980
		8	4.578	9.129	0.534	14.390	0.021	0.978

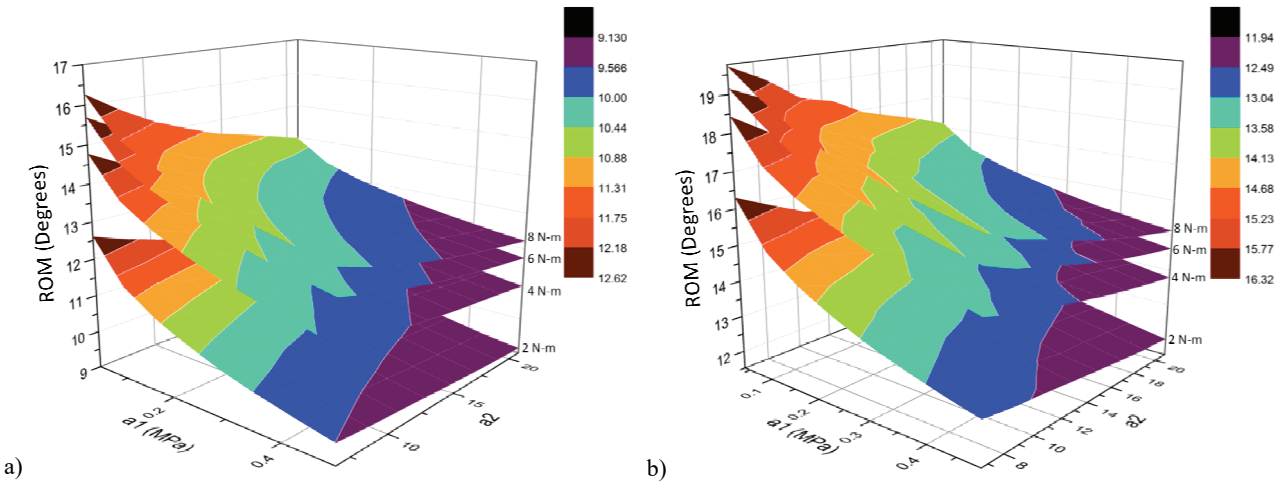

Fig. 6. Response surface of the *ROM* versus a_1 and a_2 for different magnitude of moment (represented in the legend in Nm) in flexion: a) L4-L5 disc, b) L5-S1 disc

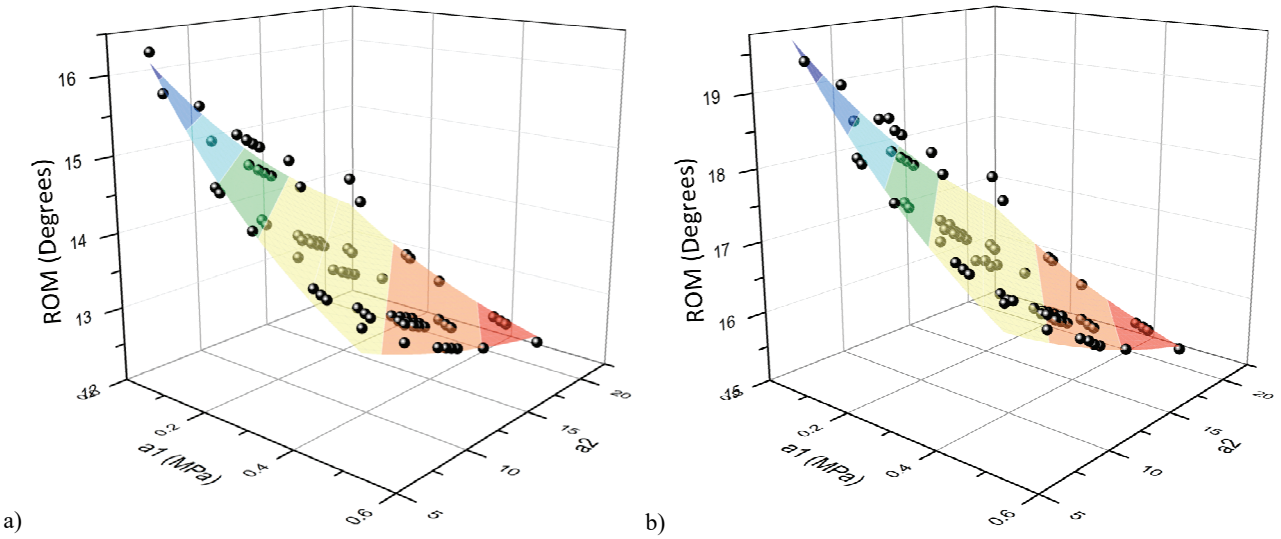

Fig. 7. *ROM* versus a_1 and a_2 in flexion under 8 Nm: a) L4-L5 disc, b) L5-S1 disc.
The black points are results of the parametric analysis and the surface represents the equation fit

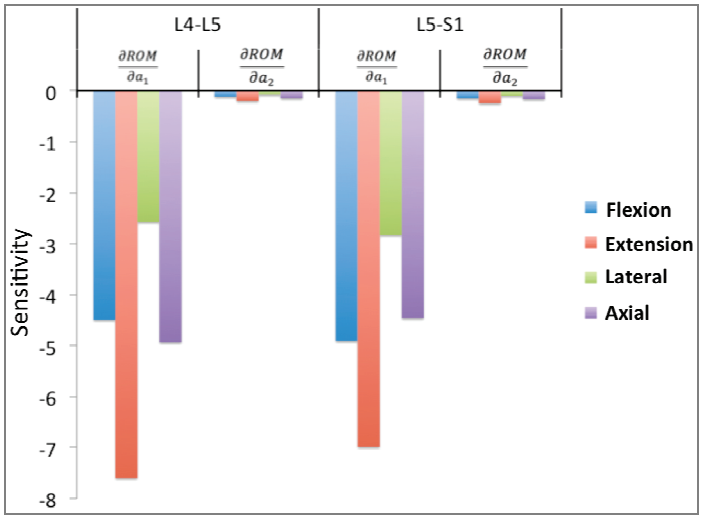

Fig. 8. *ROM* sensitivity to the a_1, a_2 coefficients

Table 4. *ROM* (in degrees) with the higher probability of occurrence

Movement	L4-L5		L5-S1	
	ROM	Probability of occurrence	*ROM*	Probability of occurrence
Flexion	12.75–13.75°	68.1%	15.75–16.75°	57.7%
Extension	10.5–11.5°	63.9%	12.5–13.5°	51.4%
Lateral flexion	5.3–6.3°	79.2%	4.75–5.75°	80.6%
Axial Rotation	5.75–6.75°	58.3%	6.25–7.25°	59.7%

The probability functions under the 8 Nm moment of force (Table 4) show that, with respect to the L4-L5 *ROM*, the *ROM* for the L5-S1 segment has a higher probability of being greater in flexion, extension and axial rotation, and lower in lateral flexion. Only the *ROM* cumulative probability density function and probability graphs are shown for flexion movement for the L4-L5 segment (Fig. 9a) and for the L5-S1 segment (Fig. 9b) for clarity.

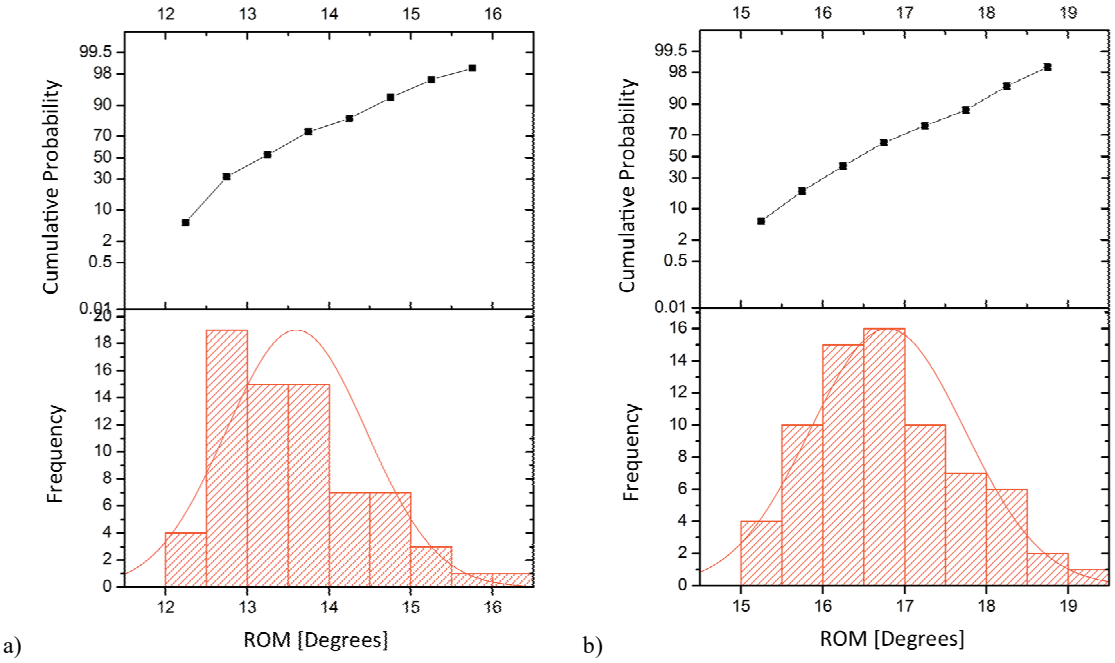

Fig. 9. *ROM* cumulative probability function and frequency in flexion under 8 Nm: a) L4-L5 disc, b) L5-S1 disc

4. Discussion

The high level of uncertainty in the geometrical parameters and mechanical properties of the annulus generates a significant dispersion in the biomechanical response. The models being analyzed show a wide dispersion patterns that cannot be described using a deterministic approach [18].

An excellent fit (R^2 = 0.98) to ROM response versus a_1 and a_2 was obtained using an analytical surface. For this reason, the equations describing theses surfaces can be used to facilitate the calibration process of finite element models that include the annulus fibrosus. The relatively high percentage of the theoretical *ROM* (97.9% in flexion, 32.0% in extension, 44.0% in lateral flexion and 59.9% in axial rotation) that was within the experimental ranges suggests that the values of a_1 and a_2 reported by Cortes et al. [4], which were used to select the set of input data for analysis, are reliable to be used in finite element models. On the other hand, lower percentage of simulation data within the experimental range for other movements may be due to the homogeneous properties used for the annulus. Other studies [3], [4], [8], [9], [32], [33] have documented property variations in the circumferential and radial directions, which may have more effect in some movements than in others. Results also indicate that in the calibration process of a finite element model, the constant a_1 should be fit first, and next a_2, because the *ROM* is more sensitive to a_1. Therefore, it is necessary to point out that a_1 defines the initial slope and a_2 define the degree of non-linear response in the stress/strain curve of the fibers.

Many finite element models [6], [10], [11], [20], [31] choose the annulus fibrosus elastic properties without performing a calibration process using experimental data. As the annulus fibrosus is one of the main elements to support lumbar load and confine the nucleus, the calibration of its properties using ROM data of a reduced segment should be the first step in the validation process of a segment model. An incorrect calibration of the annulus fibrosus constants may generate overload in other elements of the segment such as ligaments and facet joints, as shown in other studies [23].

With respect to the simplification of the vertebrae and the endplates as rigid bodies, a previous study [5] indicated that the maximum stress and the intradiscal pressure only changed of about 2% compared to the results of an elastic model for the bones and endplates. The rigid-body assumption is also adopted in the recent model reported by Moramarco et al. [17] and Cegoñino et al. [2].

5. Conclusions

The *ROM* was more sensitive to a_1 than to a_2 and, in relation to movement of the segment, the ROM was

more sensitive to the input variables in the following order: extension, flexion, axial rotation and lateral bending. Then, if calibration of a finite element model of the segment were needed it would be necessary first to fit a_1 and to use the flexion movement. Therefore, an equation is proposed to obtain the ROM as a function of the elastic constants of the fibers and the type of movement. This equation may be used to facilitate the calibration process of the human spine segments.

Acknowledgements

The authors appreciate the support of the Universidad del Valle and the Universidad Autónoma de Occidente (Cali-Colombia).

References

[1] AYTURK U.M., GARCIA J.J., PUTTLITZ C.M., *The Micromechanical Role of the Annulus Fibrosus Components Under Physiological Loading of the Lumbar Spine*, J. Biomech Eng., 2010, 132, 061007–061007.

[2] CEGOÑINO J., MORAMARCO V., CALVO-ECHENIQUE A., PAPPALETTERE C., PÉREZ DEL PALOMAR A., *A Constitutive Model for the Annulus of Human Intervertebral Disc: Implications for Developing a Degeneration Model and Its Influence on Lumbar Spine Functioning*, J. of Appl. Mathematics, 2014, e658719.

[3] CORTES D.H., ELLIOTT D.M., *Extra-fibrillar matrix mechanics of annulus fibrosus in tension and compression*, Biomech. Model Mechanobiol., 2012, 11, 781–790.

[4] CORTES D.H., HAN W.M., SMITH L.J., ELLIOTT D.M., *Mechanical properties of the extra-fibrillar matrix of human annulus fibrosus are location and age dependent*, J. of Orthop. Res., 2013, 1725–1732.

[5] DIAZ C.A., GARCÍA J.J. PUTTLITZ C., *Influence of vertebra stiffness in the finite element analysis of the intervertebral disc*, ASME, Fajarado, Puerto Rico, USA, 2012, 2.

[6] DREISCHARF M., ZANDER T., SHIRAZI-ADL A., PUTTLITZ C.M., ADAM C.J., CHEN C.S., GOEL V.K., KIAPOUR A., KIM Y.H., LABUS K.M., LITTLE J.P., PARK W.M., WANG Y.H., WILKE H.J., ROHLMANN A., SCHMIDT H., *Comparison of eight published static finite element models of the intact lumbar spine: Predictive power of models improves when combined together*, J. of Biomech., 2014, 47, 1757–1766.

[7] FAGAN M.J., JULIAN S., SIDDALL D.J., MOHSEN A.M., *Patient-specific spine models.* Part 1: *Finite element analysis of the lumbar intervertebral disc – a material sensitivity study*, Proceedings of the Institution of Mechanical Engineers, Part H: J. of Engineering in Medicine, 2002, 216, 299–314.

[8] FUJITA Y., DUNCAN N.A., LOTZ J.C., *Radial tensile properties of the lumbar annulus fibrosus are site and degeneration dependent*, J. of Orthop. Res., 1997, 15, 814–819.

[9] GREEN T.P., ADAMS M.A., DOLAN P., *Tensile properties of the annulus fibrosus*, Eur. Spine J., 1993, 2, 209–214.

[10] GUAN Y., YOGANANDAN N., ZHANG J., PINTAR F.A., CUSICK J.F., WOLFLA C.E., MAIMAN D.J., *Validation of a clinical finite element model of the human lumbosacral spine*, Med. Bio. Eng. Comput., 2006, 44, 633–641.

[11] GUO L.-X., *Finite Element Model of Spine Lumbosacral Joint and its Validation*, Chinese J. of Biom. Eng., 2006, 25, 426–429.

[12] JARAMILLO H.E., GARCÍA J.J., GÓMEZ L., *A finite element model of the L4-L5-S1 human spine segment including the heterogeneity and anisotropy of the discs*, Acta Bioeng. Biomech., 2015, 17.

[13] JARAMILLO H.E., PUTTLITZ C.M., MCGILVRAY K., GARCÍA J.J., *Characterization of the L4-L5-S1 motion segment using the stepwise reduction method*, J. Biomech., 2016, 49, 1248–1254.

[14] LAZ P.J., BROWNE M., *A review of probabilistic analysis in orthopaedic biomechanics*, Proceedings of the Institution of Mechanical Engineers, Part H: J. of Eng. in Medicine, 2010, 224, 927–943.

[15] MADSEN H.O., KRENK S., LIND N.C., *Methods of Estructural Safety*, Dover Publications Inc., United States of America, 1986.

[16] MALANDRINO A., PLANELL J.A., LACROIX D., *Statistical factorial analysis on the poroelastic material properties sensitivity of the lumbar intervertebral disc under compression, flexion and axial rotation*, J. of Biomech., 2009, 42, 2780–2788.

[17] MORAMARCO V., PÉREZ DEL PALOMAR A., PAPPALETTERE C., DOBLARÉ M., *An accurate validation of a computational model of a human lumbosacral segment*, J. of Biomech., 2010, 43, 334–342.

[18] NIEMEYER F., WILKE H.-J., SCHMIDT H., *Geometry strongly influences the response of numerical models of the lumbar spine – A probabilistic finite element analysis*, J. of Biomech., 2012, 45, 1414–1423.

[19] O'CONNELL G.D., GUERIN H.L., ELLIOTT D.M., *Theoretical and Uniaxial Experimental Evaluation of Human Annulus Fibrosus Degeneration*, J. Biomech. Eng., 2009, 131, 111007.

[20] PRENDERGAST P., *Finite element models in tissue mechanics and orthopaedic implant design*, Clinical Biomechanics, 1997, 12, 343–366.

[21] RAO A.A., DUMAS G.A., *Influence of material properties on the mechanical behaviour of the L5-S1 intervertebral disc in compression: a nonlinear finite element study*, J. of Biomed. Eng., 1991, 13, 139–151.

[22] ROHLMANN A., MANN A., ZANDER T., BERGMANN G., *Effect of an artificial disc on lumbar spine biomechanics: a probabilistic finite element study*, Eur. Spine J., 2009, 18, 89–97.

[23] SCHMIDT H., HEUER F., SIMON U., KETTLER A., ROHLMANN A., CLAES L., WILKE H.-J., *Application of a new calibration method for a three-dimensional finite element model of a human lumbar annulus fibrosus*, Clin. Biomech., 2006, 21, 337–344.

[24] SHIN D.S., LEE K., KIM D., *Biomechanical study of lumbar spine with dynamic stabilization device using finite element method*, Computer-Aided Design., 2007, 39, 559–567.

[25] SPILKER R.L., *Mechanical behavior of a simple model of an intervertebral disk under compressive loading*, J. of Biomech., 1980, 13, 895–901.

[26] SPILKER R.L., DAUGIRDA D.M., SCHULTZ A.B., *Mechanical response of a simple finite element model of the intervertebral disc under complex loading*, J. of Biomech., 1984, 17, 103–112.

[27] SPILKER R.L., JAKOBS D.M., SCHULTZ A.B., *Material constants for a finite element model of the intervertebral disk*

with a fiber composite annulus, J. of Biomech. Eng., 1986, 108, 1–11.

[28] THACKER B., NICOLELLA D., *Probabilistic Finite Element Analysis of the Human Lower Cervical Spine*, Abaqus., 2013, 1, 1–12.

[29] THACKER B., WU Y.-T., NICOLELLA D., ANDERSON R., THACKER B., NICOLELLA D., ANDERSON R., *Probabilistic injury analysis of the cervical spine*, American Institute of Aeronautics and Astronautics, 1997.

[30] ŁODYGOWSKI T., KĄKOL W., WIERSZYCKI M., *Three-dimensional nonlinear finite element model of lumbar intervertebral disc*, Acta Bioeng. Biomech., 2005, 7, 29–37.

[31] YOGANANDAN N., MYKLEBUST J.B., RAY G., PINTAR F., SANCES A. Jr., *A non-linear finite element model of a spinal segment*, Mathematical Modelling, 1987, 8, 617–622.

[32] ŻAK M., PEZOWICZ C., *Spinal sections and regional variations in the mechanical properties of the annulus fibrosus subjected to tensile loading*, Acta Bioeng. Biomech., 2013, 15, 51–59.

[33] ZHU D., GU G., WU W., GONG H., ZHU W., JIANG T., CAO Z., *Micro-structure and mechanical properties of annulus fibrous of the L4-5 and L5-S1 intervertebral discs*, Clinical Biomech., 2008, 23, Suppl. 1, S74–S82.